

Hydration of potassium iodide dimer studied by photoelectron spectroscopy and *ab initio* calculations

Ren-Zhong Li,^{1,2} Zhen Zeng,³ Gao-Lei Hou,³ Hong-Guang Xu,³ Xiang Zhao,^{1,a)}
 Yi Qin Gao,^{4,a)} and Wei-Jun Zheng^{3,a)}

¹Institute for Chemical Physics, School of Science, Xi'an Jiaotong University, Xi'an 710049, China

²College of Electronics and Information, Xi'an Polytechnic University, Xi'an 710048, China

³Beijing National Laboratory for Molecular Sciences, State Key Laboratory of Molecular Reaction Dynamics, Institute of Chemistry, Chinese Academy of Sciences, Beijing 100190, China

⁴Beijing National Laboratory for Molecular Sciences, Institute of Theoretical and Computational Chemistry, College of Chemistry and Molecular Engineering, Peking University, Beijing 100871, China

(Received 20 September 2016; accepted 12 October 2016; published online 14 November 2016)

We measured the photoelectron spectra of $(\text{KI})_2^-(\text{H}_2\text{O})_n$ ($n = 0-3$) and conducted *ab initio* calculations on $(\text{KI})_2^-(\text{H}_2\text{O})_n$ anions and their corresponding neutrals up to $n = 6$. Two types of spectral features are observed in the experimental spectra of $(\text{KI})_2^-(\text{H}_2\text{O})$ and $(\text{KI})_2^-(\text{H}_2\text{O})_2$, indicating that two types of isomers coexist, in which the high EBE feature corresponds to the hydrated chain-like $(\text{KI})_2^-$ while the low EBE feature corresponds to the hydrated pyramidal $(\text{KI})_2^-$. In $(\text{KI})_2^-(\text{H}_2\text{O})_3$, the $(\text{KI})_2^-$ unit prefers a pyramidal configuration, and one of the K–I distances is elongated significantly, thus a K atom is firstly separated out from the $(\text{KI})_2^-$ unit. As for the neutrals, the bare $(\text{KI})_2$ has a rhombus structure, and the structures of $(\text{KI})_2(\text{H}_2\text{O})_n$ are evolved from the rhombus $(\text{KI})_2$ unit by the addition of H_2O . When the number of water molecules reaches 4, the K–I distances have significant increment and one of the I atoms prefers to leave the $(\text{KI})_2$ unit. The comparison of $(\text{KI})_2(\text{H}_2\text{O})_n$ and $(\text{NaI})_2(\text{H}_2\text{O})_n$ indicates that it is slightly more difficult to pry apart $(\text{KI})_2$ than $(\text{NaI})_2$ via hydration, which is in agreement with the lower solubility of KI compared to that of NaI. *Published by AIP Publishing.* [<http://dx.doi.org/10.1063/1.4967168>]

I. INTRODUCTION

Dissolution of salts plays an important role in many processes in physical chemistry, atmospheric chemistry, biochemical, and biological systems.¹⁻³ The salt effects on water are strongly correlated to the much discussed Hofmeister series.⁴⁻¹¹ The group IA cations are ordered as H^+ , Li^+ , Na^+/K^+ , Rb^+ , Cs^+ in the Hofmeister series according to their sizes and surface charge densities.¹² The ions on the left side of this series can be strongly hydrated due to their small sizes and high surface charge densities, whereas those on the right side can be weakly hydrated owing to their large sizes and low surface charge densities.^{12,13} The hydration of K^+ is crucial for understanding the salt effects on water in the Hofmeister series because it is believed that the switch from Na^+ to K^+ is a transition point between kosmotropes (structure makers) and chaotropes (structure breakers). In addition, it has been found that the hydration and dehydration processes are important in the transportation of K^+ ions through the cavity of the potassium ion channel in the cell membranes.¹⁴ Thus, the solvation of K^+ and potassium salts has attracted great attention in the past decades.

Many theoretical studies were performed to investigate the solvation of K^+ . The structures, thermodynamic energies,

and IR spectra of $\text{K}^+(\text{H}_2\text{O})_{16}$ clusters¹⁵ as well as the molecular polarization in the hydration clusters of alkali metal ions (Li^+ , Na^+ , K^+)¹⁶ were studied by theoretical calculations. The solvation structures of K^+ and other salt ions in aqueous solution were investigated with *ab initio* molecular dynamics.¹⁷⁻²⁰ The charge-transfer-to-solvent (CTS) transitions of I^- ion and K^+I^- contact ion pair in supercritical ammonia at 420 K were studied employing the Hartree-Fock (HF) method, Møller-Plesset second order perturbation theory (MP2), and single-excitation configuration interaction (CIS) method combining a molecular dynamics trajectory-sampling technique.²¹ The hydrated potassium halides, such as $\text{KX}(\text{H}_2\text{O})_{1-6}$ ($\text{X} = \text{F}, \text{Cl}, \text{Br}, \text{I}$), were investigated with *ab initio* calculations.²² In addition to the theoretical works, there were abundant experimental works. The hydration of K^+ in aqueous solutions was explored in the condensed phases with a variety of experimental techniques such as neutron diffraction,²³⁻²⁵ extended X-ray absorption fine structure spectroscopy (EXAFS),²⁶ large angle X-ray scattering (LAXS),²⁷ soft X-ray emission spectroscopy,²⁸ X-ray diffraction, and Raman spectroscopy.^{29,30} The vibrational frequencies of $\text{M}(\text{H}_2\text{O})$ complexes ($\text{M} = \text{Na}, \text{K}, \text{and Cs}$) were measured employing matrix-isolated infrared spectroscopy.³¹ The hydration energies of $(\text{MX})_m\text{M}^+$ ions including KXK^+ ($\text{X} = \text{F}^-, \text{Br}^-, \text{I}^-$) with up to four water molecules were investigated using electrospray ionization mass spectrometry and density functional theory calculations.³² The hydration of K^+ and the other alkali-metal cations were studied in the

^{a)}Authors to whom correspondence should be addressed. Electronic addresses: zhengwj@iccas.ac.cn; xzhao@mail.xjtu.edu.cn; and gaoyq@pku.edu.cn. Telephone: +86 10 62635054. Fax: +86 10 62563167.

gas phase via infrared photodissociation spectroscopy.^{33–35} Previously, we conducted a photoelectron spectroscopy and theoretical study on the hydration of sodium iodide dimer.³⁶ In this work, in order to provide a comparison between sodium iodide dimer and potassium iodide dimer and to help understand why K^+ plays a different role in solutions and biological systems, we conducted a combined experimental and theoretical study on $(KI)_2^-(H_2O)_n$ clusters and their corresponding neutrals by negative ion photoelectron spectroscopy and *ab initio* calculations.

II. EXPERIMENTAL AND THEORETICAL METHODS

A. Experimental methods

The experiments were carried out using a home-built apparatus consisting of a time-of-flight (TOF) mass spectrometer and a magnetic-bottle photoelectron spectrometer, which has been described elsewhere.³⁷ In the experiment, a rotating and translating KI disk target was ablated by the second harmonic (532 nm) light pulses from a Nd:YAG laser, while helium carrier gas with ~ 4 atm backing pressure seeded with water vapor was allowed to expand through a pulsed valve to generate and cool the hydrated potassium iodide clusters. The $(KI)_2^-(H_2O)_n$ ($n = 0-3$) clusters were each mass-selected and decelerated before being photodetached by the 532 nm photons from another Nd:YAG laser. The photodetached electrons were energy-analyzed by the magnetic-bottle photoelectron spectrometer. The photoelec-

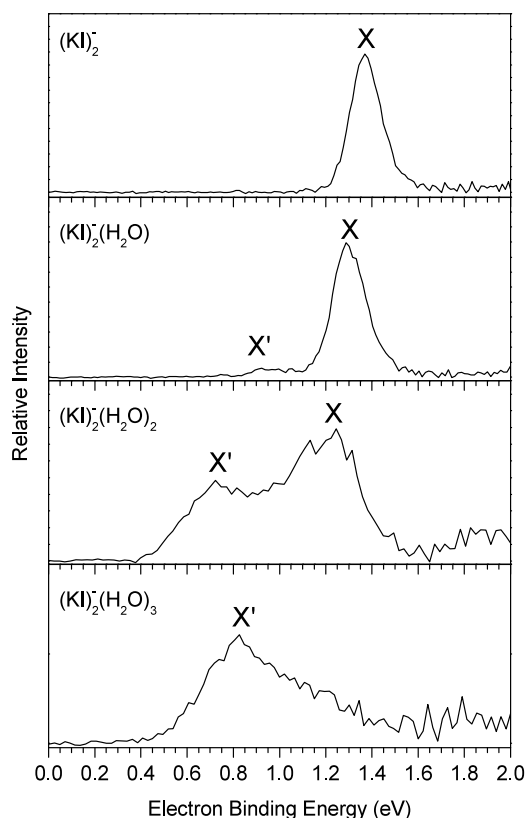


FIG. 1. Photoelectron spectra of $(KI)_2^-(H_2O)_n$ ($n = 0-3$) clusters measured with 532 nm photons.

TABLE I. Experimentally observed ADEs and VDEs of $(KI)_2^-(H_2O)_n$ ($n = 0-3$) from their photoelectron spectra.

Cluster	X'		X	
	ADE (eV)	VDE (eV)	ADE (eV)	VDE (eV)
$(KI)_2^-$			1.22 ± 0.08	1.37 ± 0.08
$(KI)_2^-(H_2O)$	0.83 ± 0.10	0.93 ± 0.10	1.15 ± 0.08	1.28 ± 0.08
$(KI)_2^-(H_2O)_2$	0.43 ± 0.10	0.72 ± 0.10	0.77 ± 0.10	1.22 ± 0.08
$(KI)_2^-(H_2O)_3$	0.51 ± 0.08	0.82 ± 0.10		

tron spectra were calibrated with the spectra of Cs^- and Bi^- taken at similar conditions. The instrumental resolution was approximately 40 meV for electrons with 1 eV kinetic energy.

B. Theoretical methods

The theoretical calculations were conducted using the Gaussian 09 program package.³⁸ The geometries of $(KI)_2^-(H_2O)_n$ and their neutrals were fully optimized using density functional theory (DFT) in the context of LC- ω PBE (a long-range corrected hybrid functional).^{39–41} The typical low-lying structures of $(KI)_2^-(H_2O)_{1-6}$ clusters were further optimized using the second-order Møller-Plesset (MP2)^{42–45} method. The Pople's all-electron basis set 6-311++G(d, p) was used for the K, O, and H atoms. The *ab initio* effective core potential (ECP) basis set LANL2DZdp⁴⁶ obtained from the EMSL basis set library⁴⁷ was used for the I atoms. The optimized structures were confirmed to be real minima by calculations of their second derivatives. The theoretical vertical detachment energies (VDEs) were obtained as the energy differences between the neutrals and anions both at the geometries of the anions. The theoretical adiabatic detachment energies (ADEs) were calculated as the energy differences between the neutrals and anions with the neutrals relaxed to the nearest local minima from the geometries of the anions. To get more accurate energetic information, we performed single-point energy calculations

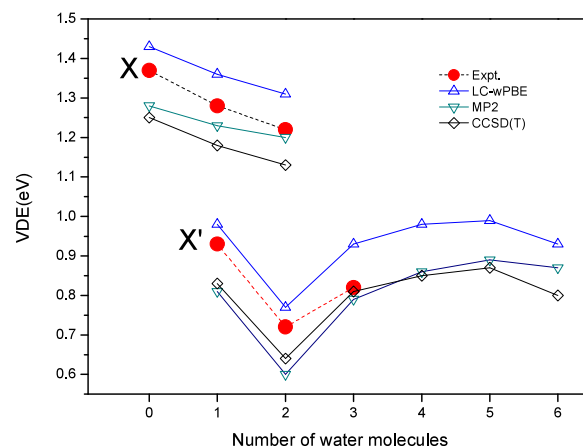


FIG. 2. Comparison of the theoretical VDEs of the most stable isomers of $(KI)_2^-(H_2O)_n$ ($n = 0-6$) with the experimental VDEs.

for the $(\text{KI})_2^{-/0}(\text{H}_2\text{O})_{0-6}$ clusters with high-level *ab initio* CCSD(T)^{48,49} method at LC- ω PBE optimal geometries using the def2-TZVPP basis set⁵⁰ from the EMSL basis set library for I atoms. Additionally, to better understand the interactions between cations, anions, and water, the bonding and electronic properties were also explored using the atoms-in-molecules (AIM) approach,^{51,52} and a visual study performed by calculating the reduced density gradient (RDG).⁵³ The AIM and RDG were analysed by using the Multiwfn program.⁵⁴

III. EXPERIMENTAL RESULTS

Figure 1 shows the photoelectron spectra of $(\text{KI})_2^{-}(\text{H}_2\text{O})_n$ ($n = 0-3$) clusters measured with 532 nm photons. The VDEs

and ADEs of these clusters measured from their spectra are summarized in Table I. We were not able to obtain the photoelectron spectra of $(\text{KI})_2^{-}(\text{H}_2\text{O})_n$ with $n > 3$ due to the low ion intensities of $(\text{KI})_2^{-}(\text{H}_2\text{O})_n$ and the overlap of the mass peaks with impurities.

Only one major peak centered at about 1.37 eV is observed in the spectrum of $(\text{KI})_2^{-}$, consistent with the previous reports.^{55,56} The spectrum of $(\text{KI})_2^{-}(\text{H}_2\text{O})$ has a weak peak (X') centered at ~ 0.93 eV and a major peak (X) at 1.28 eV. These two bands may be contributed by two types of isomers, respectively. The spectrum of $(\text{KI})_2^{-}(\text{H}_2\text{O})_2$ has also two peaks centered at ~ 0.72 (X') and 1.22 eV (X), respectively. The relative intensity of the X' peak versus X peak increases when the number of water molecules increases from one to two, indicating that the relative ion intensity of the isomer contributing to the X' peak increases. The spectrum of

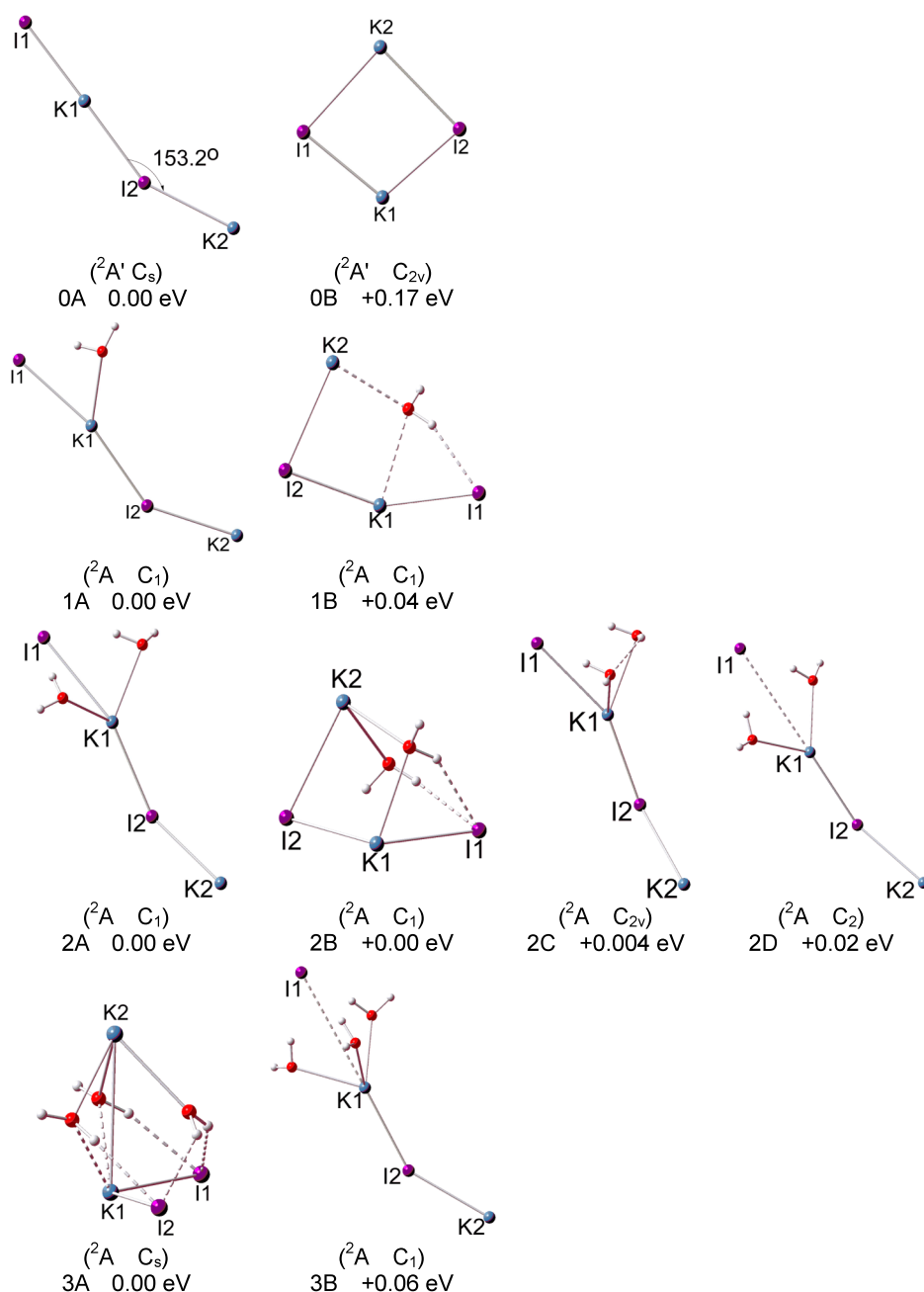


FIG. 3. Typical low-lying isomers of $(\text{KI})_2^{-}(\text{H}_2\text{O})_n$ ($n = 0-3$) clusters.

$(\text{KI})_2^-(\text{H}_2\text{O})_3$ shows only one broad feature (X') centered at about 0.82 eV, and the X peak at the higher binding energy side becomes almost unrecognizable, suggesting that the isomer corresponding to the X peak is much less populated. The change of VDEs versus n is summarized and compared with that of theoretical VDEs in Figure 2. It can be seen that the VDE of the X peak decreases when n increases from 0 to 2. The VDE of the X' peak drops at $n = 2$, then rises up at $n = 3$.

IV. THEORETICAL RESULTS AND DISCUSSION

A. Structures of $(\text{KI})_2^-(\text{H}_2\text{O})_n$ and $(\text{KI})_2(\text{H}_2\text{O})_n$ ($n = 0-6$)

The structures of the typical low-lying isomers of $(\text{KI})_2^-(\text{H}_2\text{O})_n$ optimized with the MP2 method are presented in Figures 3 and 4, and those of the neutral clusters are shown in Figures 5 and 6. The theoretical relative energies and VDEs of these low-lying isomers are listed in Table II. It is worth

mentioning that, in Figure 2, the theoretical VDEs calculated at different levels of theory are in good agreement with the experimental values.

The geometry optimizations at the MP2 level of theory show that the global minimum of $(\text{KI})_2^-(0\text{A})$ is in ${}^2\text{A}'$ state and has a C_s symmetry chain structure with a $\angle\text{KIK}$ angle of 153.2° . We further optimized the structure of $(\text{KI})_2^-$ with the CCSD method and found that the structure is same as that obtained with the MP2 method, indicating the structure optimized with the MP2 method is reliable. The theoretical VDE of $(\text{KI})_2^-$ is calculated to be 1.28 eV with both MP2 and CCSD methods, close to the experimental value of 1.37 eV measured in this work. Isomer 0B is higher than 0A by 0.17 eV and it is a ring structure with C_{2v} symmetry and ${}^2\text{A}'$ state. The calculated VDE of 0B is 0.26 eV, much different from the experiment measurement. Therefore, isomer 0A is the one detected in the experiment. For $(\text{KI})_2$ neutral, the most stable structure 0A' is a rhombus with D_{2h} symmetry and the K-I distance is calculated to be 3.34 Å with both MP2

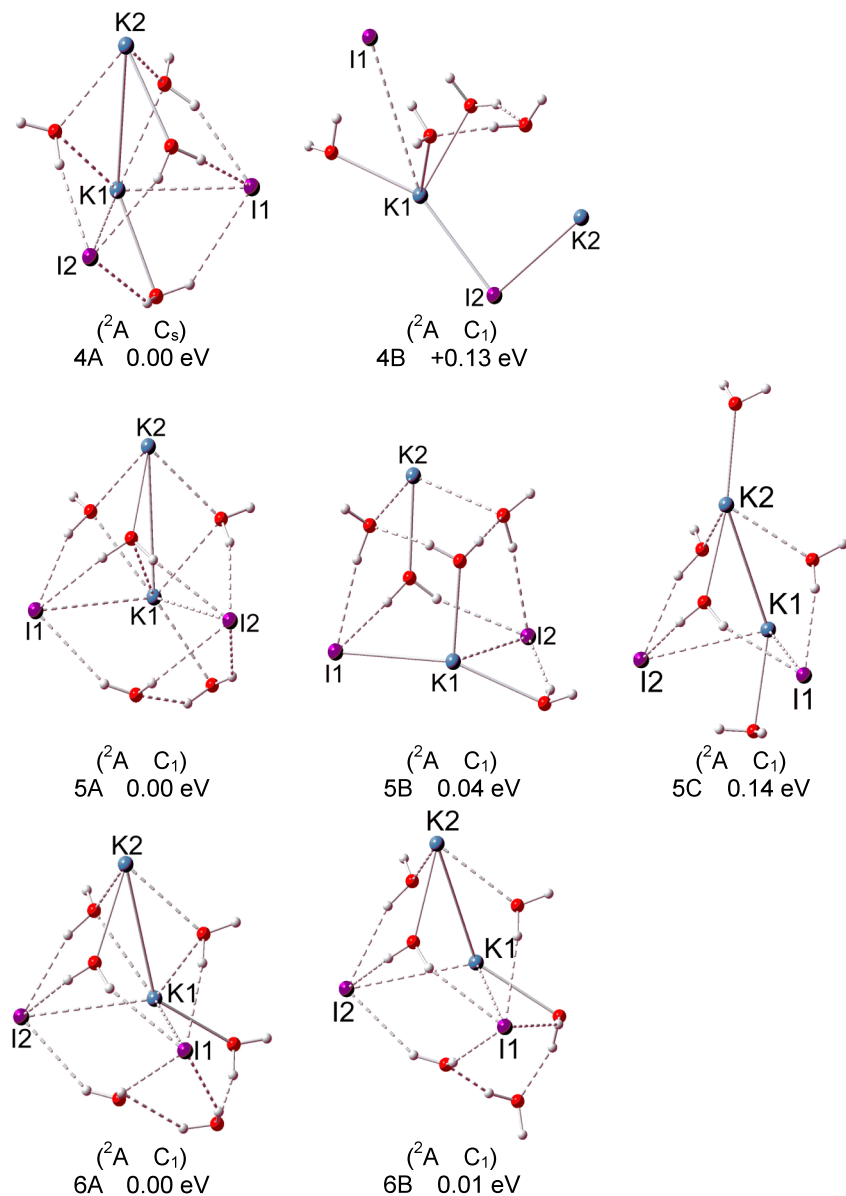


FIG. 4. Typical low-lying isomers of $(\text{KI})_2^-(\text{H}_2\text{O})_n$ ($n = 4-6$) clusters.

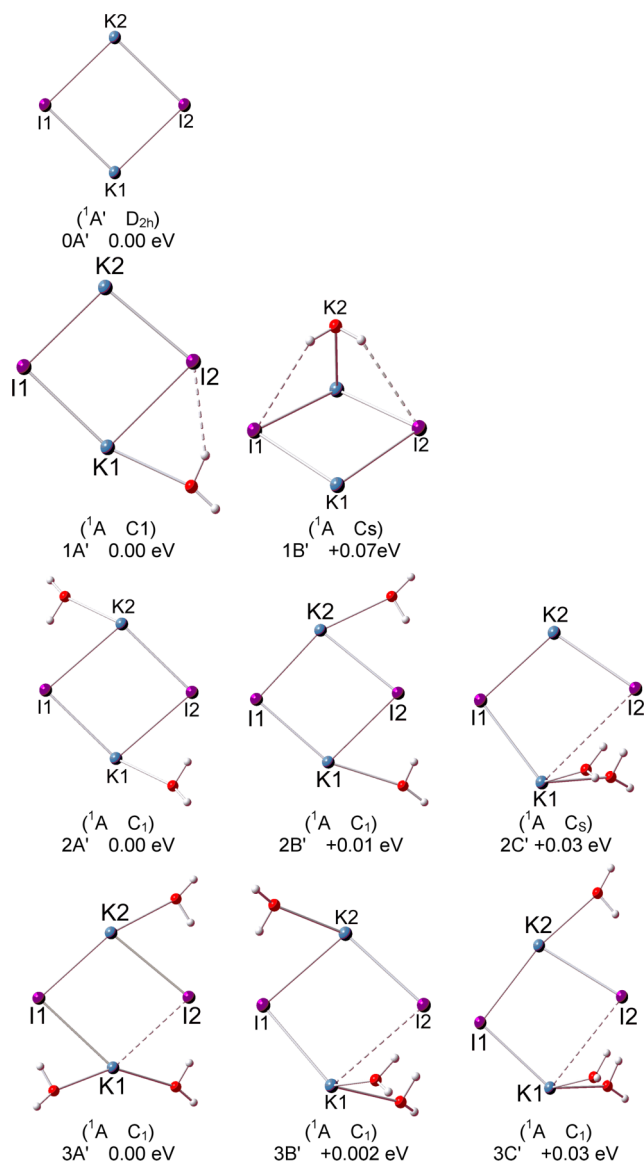


FIG. 5. Typical low-lying isomers of $(\text{KI})_2(\text{H}_2\text{O})_n$ ($n=0-3$) clusters.

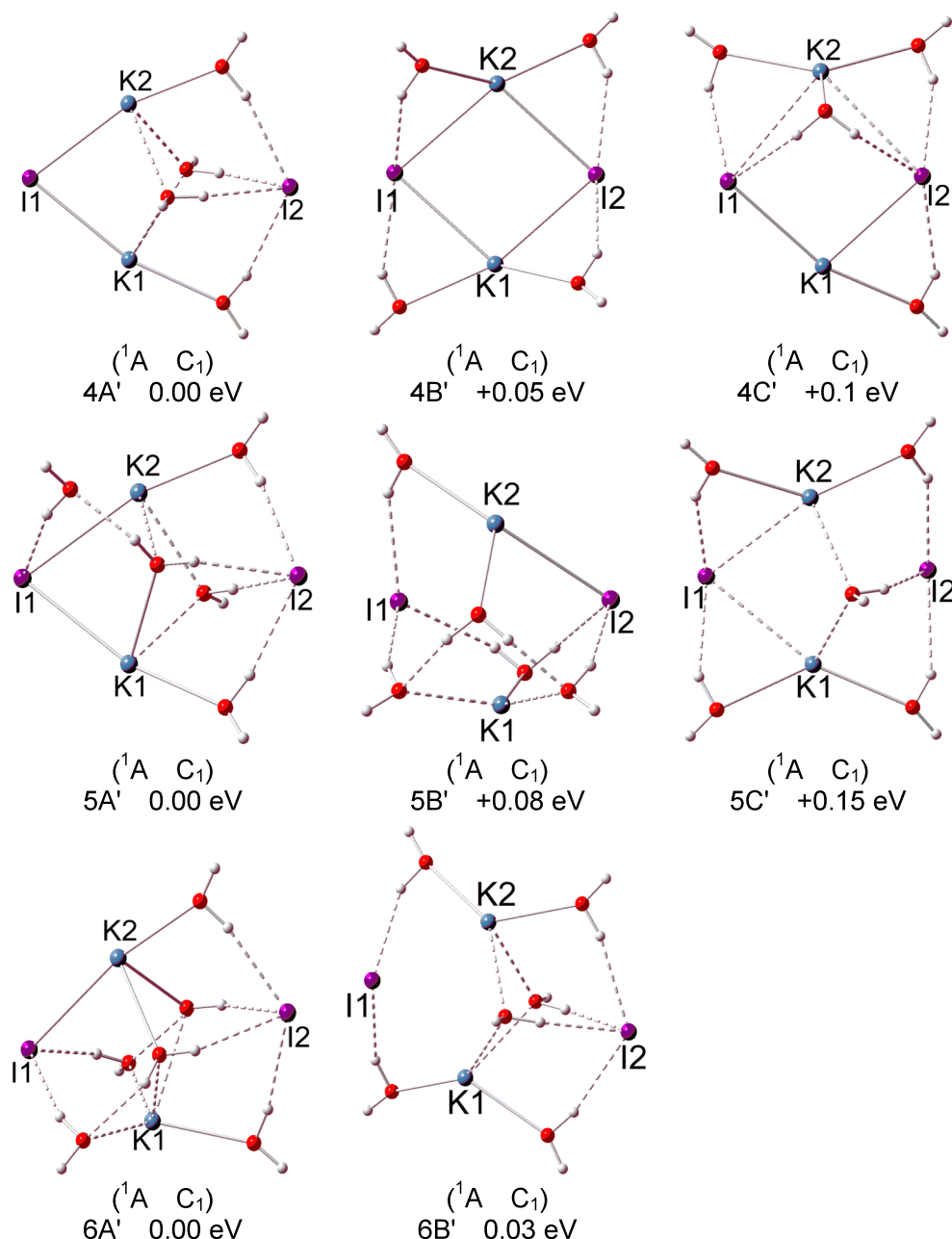
and CCSD methods, in agreement with previous theoretical calculations.⁵⁶

The most stable structure of $(\text{KI})_2^-(\text{H}_2\text{O})$ was formed via the chain shaped $(\text{KI})_2^-$ attaching one water molecule by K1–O and I1–H interactions. The K1–I1 distance is longer than that in bare $(\text{KI})_2^-$ by 0.17 Å. The calculated VDE (1.23 eV) with the MP2 method agrees well with the experimental VDE (1.28 eV) of the second peak (X). We note that $(\text{KI})_2^-$ attaching one water molecule brings a lower VDE, the phenomenon has also been found in $(\text{NaI})_2^-(\text{H}_2\text{O})_n$ ³⁶ and may be explained by the similar reason. Isomer 1B is higher in energy than isomer 1A by only 0.04 eV. In isomer 1B, the K1–I2–K2 is bent with a $\angle\text{K1I2K2}$ angle of 81.2°, the water molecule interacts with both K1 and K2 atoms via its O atom, and one of its H atoms forms a hydrogen bond with I1. The calculated VDE of 1B is 0.81 eV at the MP2 level, close to the experimental VDE of the X' peak (0.93 eV) in our experiment. Thus, isomer 1B mainly contributes to the weak X' peak. For the neutral $(\text{KI})_2(\text{H}_2\text{O})$, the first two low-lying isomers are

derived from the rhombus $(\text{KI})_2(0\text{A}')$. Isomer 1A' is formed by adding a water molecule to the rhombus $(\text{KI})_2$ with the O atom of H_2O interacting with the K1 atom and a O–H group of H_2O forms a hydrogen bond with I2 atom. Isomer 1B' is higher in energy than 1A' by 0.07 eV. It is formed by attaching a water molecule above the plane of rhombus $(\text{KI})_2$ with the O atom of H_2O interacting with one K atom and the O–H groups of H_2O form two hydrogen bonds with the I atoms.

$(\text{KI})_2^-(\text{H}_2\text{O})_2$ has four isomers almost degenerate in energy with isomer 2D higher than 2A by only 0.02 eV. In isomer 2A, the two water molecules interact with both K1 and I1 with the O atoms of water molecules pointing to K1 and each H_2O forming a hydrogen bond with I1. The K1–I1 distance increases to 3.72 Å, longer than that in bare $(\text{KI})_2^-$ by 0.45 Å. The calculated VDE of 2A at the MP2 level is 1.20 eV, in good agreement with the experimental VDE of the X peak (1.22 eV) in the experimental spectrum. Isomer 2B is degenerate with 2A in energy. In isomer 2B, the $(\text{KI})_2^-$ can be considered approximately as a pyramid-shaped unit with two water molecules interacting with I2 via H atoms and interacting with the adjacent K atoms via their O atoms. The theoretical VDE of isomer 2B is calculated to be 0.60 eV, close to the VDE of the X' peak in the experimental spectrum. Isomer 2C is higher in energy than the most stable isomer by only 0.004 eV. The calculated VDE of the isomer 1.22 eV is also in agreement with the experimental VDE of the X peak (1.22 eV). In isomer 2D, the $(\text{KI})_2^-$ unit has a quasilinear structure with two water molecules inserting between K1 and I1, with the K1–I1 distance increasing to 4.82 Å. The calculated VDE of 2D is 1.29 eV, consistent with the experimental VDE of the X peak (1.22 eV) in the experimental spectrum. Therefore, the X peak in the experimental spectrum should be contributed by the chain structures such as isomers 2A, 2C, and 2D, whereas the X' peak is contributed by isomer 2B. For the neutrals, Figure 5 shows three isomers derived from the rhombus structure of $(\text{KI})_2$. In isomer 2A', the two water molecules interact with K1 and K2 via their respective O atoms and form hydrogen bonds with I1 and I2. Isomer 2B' and 2C' are higher than the global minimum (2A') by 0.01 and 0.03 eV in energy, respectively. Isomer 2B' was formed by adding two water molecules to the K2–I2 and K1–I2 edges of quadrilateral $(\text{KI})_2$ unit. In isomer 2C', the two water molecules sit between the K1–I2 unit and interact with the same K and I atoms.

For $(\text{KI})_2^-(\text{H}_2\text{O})_3$, isomer 3A has a C_s symmetry with a pyramid-shaped $(\text{KI})_2^-$ framework, with each I atom of the $(\text{KI})_2^-$ unit interacting with two H atoms of two water molecules and the K atoms interacting with the adjacent oxygen atoms. The calculated VDE of 3A is 0.79 eV, in good agreement with the X' peak (0.83 eV) in the experimental spectrum. Isomer 3B is higher in energy than 3A by 0.06 eV. It has a chain-shaped $(\text{KI})_2^-$ unit and three water molecules sitting between I1 and K1 with the H atom of water interacting with I1 atom and the O atoms of water connecting with K1. The calculated VDE of isomer 3B is 1.20 eV. From Figure 1, it can be seen that the spectrum of $(\text{KI})_2^-(\text{H}_2\text{O})_3$ has a very broad peak in the range of ~0.60–1.35 eV. So isomer 3B

FIG. 6. Typical low-lying isomers of $(\text{KI})_2(\text{H}_2\text{O})_n$ ($n = 4-6$) clusters.

probably contributes to the higher energy part in the spectrum of $(\text{KI})_2^-(\text{H}_2\text{O})_3$. As for the neutrals, the most stable isomer $3\text{A}'$ is formed by attaching three water molecules to the K1-I1 , K1-I2 , and K2-I2 edges of the quadrilateral $(\text{KI})_2$ unit, respectively. In isomer $3\text{B}'$, one water molecule interacts with K2-I1 and the other two water molecules sit between I1-K2 .

For $(\text{KI})_2^-(\text{H}_2\text{O})_4$, the most stable isomer 4A has a pyramid-shaped $(\text{KI})_2^-$ unit and has a C_s symmetry. It is formed by attaching an additional water molecule to 3A with K2-O interaction, and the water forms a hydrogen bond with I1 and I2 , respectively. The calculated VDE is 0.86 eV at the MP2 level. Isomer 4B is higher in energy than 4A by 0.13 eV with three water molecules sitting between K1 and I1 and the fourth water molecule forming hydrogen bonds

with the adjacent water via its O atom and one H atom. For the neutral isomers, in isomer $4\text{A}'$, four water molecules sit between I2 atom and K_2 unit. The $\text{K1}\cdots\text{I2}$ and $\text{K2}\cdots\text{I2}$ distances increase abruptly to 4.85 Å due to the interactions with water; whereas the $\text{K1}\cdots\text{I2}$ and $\text{K2}\cdots\text{I2}$ distances at another side without water molecules are 3.38 Å, almost unchanged compared with those in bare $(\text{KI})_2$ unit. Isomer $4\text{B}'$ is higher in energy than $4\text{A}'$ by 0.05 eV. It has four water molecules interacting with the four edges of $(\text{KI})_2$ rhombus, respectively.

For $(\text{KI})_2^-(\text{H}_2\text{O})_5$, three low-lying isomers are found. Isomer 5A is derived from 4A with the fifth water molecule interacting with K1 and I1 via its O atom and one H atom, respectively, and forming a water-water H-bonding with the adjacent water. The calculated VDE of 5A is 0.89 eV at the

TABLE II. Relative energies of the low energy isomers of $(\text{KI})_2^-(\text{H}_2\text{O})_n$ ($n=0-6$) as well as the comparison of their theoretical VDEs to the experimental VDEs. The 6-311++G** basis set was used for K, O, and H atoms, and the LANL2DZdp ECP basis set was used for iodine atom at LC- ω PBE and MP2 level, whereas the def2-TZVPP basis set was used for iodine atom at CCSD(T) level.

Cluster	Isomer	ΔE^a (eV)	Sym.	State	VDE (eV)			
					Theoretical			Expt.
					LC- ω PBE	MP2	CCSD(T)	
$(\text{KI})_2^-$	0A	0.00	C_s	$2A'$	1.43	1.28	1.25	1.37
	0B	0.17	C_{2v}	$2A'$	0.40	0.27	0.26	
$(\text{KI})_2^-(\text{H}_2\text{O})$	1A	0.00	C_1	$2A$	1.36	1.23	1.18	1.28
	1B	0.04	C_1	$2A$	0.98	0.81	0.83	0.93
$(\text{KI})_2^-(\text{H}_2\text{O})_2$	2A	0.00	C_1	$2A$	1.31	1.20	1.13	1.22
	2B	0.00	C_1	$2A$	0.77	0.60	0.64	0.72
	2C	0.004	C_{2v}	$2A$	1.33	1.22	1.16	
	2D	0.02	C_2	$2A$	1.40	1.29	1.23	
$(\text{KI})_2^-(\text{H}_2\text{O})_3$	3A	0.00	C_s	$2A$	0.93	0.79	0.81	0.82
	3B	0.06	C_1	$2A$	1.32	1.20	1.15	
	3C	0.10	C_1	$2A$	1.17	1.02	1.02	
$(\text{KI})_2^-(\text{H}_2\text{O})_4$	4A	0.00	C_s	$2A$	0.98	0.86	0.85	
	4B	0.13	C_1	$2A$	0.98	0.85	0.83	
$(\text{KI})_2^-(\text{H}_2\text{O})_5$	5A	0.00	C_1	$2A$	0.99	0.89	0.87	
	5B	0.04	C_1	$2A$	0.77	0.68	0.64	
	5C	0.14	C_1	$2A$	0.98	0.87	0.88	
$(\text{KI})_2^-(\text{H}_2\text{O})_6$	6A	0.00	C_1	$2A$	0.93	0.87	0.80	
	6B	0.01	C_1	$2A$	0.95	0.87	0.82	

^aThe ΔE values are from the MP2 level.

MP2 level. Isomer 5B can be considered as 3A attaching the fourth water via K1–O and I2–H interactions and attaching the fifth water via K1–O interaction and I1–H, O–H–O hydrogen bonds. Isomer 5C is formed by 4A attaching one water molecule via K2–O interaction. As for the neutral isomer, the most stable isomer 5A' is built by 4A' attaching an additional water molecule. The fifth water molecule forms two hydrogen bonds with one H atom of the nearest water via its O atom and with I1 via its one H atom.

For $(\text{KI})_2^-(\text{H}_2\text{O})_6$, the most stable structure 6A is formed by two water molecules attaching to 4A with I1–H and K1–O interactions. The two additional water molecules form two water-water hydrogen bonds via interacting with the adjacent water. Isomer 6B is also derived from 4A and only higher than 6A in energy by 0.01 eV. In isomer 6B, the fifth water was attached to 4A via I1–H and K1–O interactions and then the sixth water was added via forming hydrogen bonds with the adjacent two water molecules. The calculated VDEs of both 6A and 6B are 0.87 eV at the MP2 level. As for the neutrals of $(\text{KI})_2(\text{H}_2\text{O})_6$, two isomers almost degenerate in energy (6A' and 6B') are found. In isomer 6A', four water molecules sit between I2 and K2 unit and the other two water molecules sit between I1 and K1. The K1–I2 and K2–I2 distances are 4.77 and 4.68 Å respectively, and the K1–I1 and K2–I1 distances are 3.67 Å and 3.49 Å respectively. Isomer 6B' is derived from 4A' with the additional two water molecules sitting between K1–I1 and K2–I1, respectively.

B. Ion separation in $(\text{KI})_2^-(\text{H}_2\text{O})_n$ and $(\text{KI})_2(\text{H}_2\text{O})_n$

In the most stable structure of bare $(\text{KI})_2^-$, the I1–K1, I2–K1, and I2–K2 distances are 3.27, 3.37, and 3.42 Å respectively. The I1–K1 distance increases slightly by 0.17 and 0.45 Å in $(\text{KI})_2^-(\text{H}_2\text{O})_1$ and $(\text{KI})_2^-(\text{H}_2\text{O})_2$. When the number of water molecules increase to three, the distances between the K atom at apex and the two I atoms in the pyramid-shaped structures are both 5.32 Å, and have a significant elongation comparing with the K–I distances of the bare $(\text{KI})_2^-$, indicating that the apex K atom is separated out from the pyramid-shaped $(\text{KI})_2^-$ unit. For the neutrals, the K1–I2 and K2–I2 distances increased to 4.86 Å as the number of water molecules increases to 4, indicating that one I[−] ion can be first separated out from the $(\text{KI})_2$ unit by 4 water molecules.

The natural populations analysis (NPA) shows that the NPA charge on K2 in neutral $(\text{KI})_2(\text{H}_2\text{O})_n$ is in the range of +0.966 to +0.985 e, whereas that on K2 in the corresponding anion $(\text{KI})_2^-(\text{H}_2\text{O})_n$ is from −0.036 to −0.021 e. This indicates that the excess electron of $(\text{KI})_2^-(\text{H}_2\text{O})_n$ is mainly localized on K2. In order to show clearly the variation of electron density, we also analyzed electron density differences between the anions and their corresponding neutrals using Multiwfn software. The electron density difference isosurfaces were produced by subtracting the electron densities of neutrals from those of anions (Figure 7). It can be seen that there are high local blue regions near K2, indicating that the electron

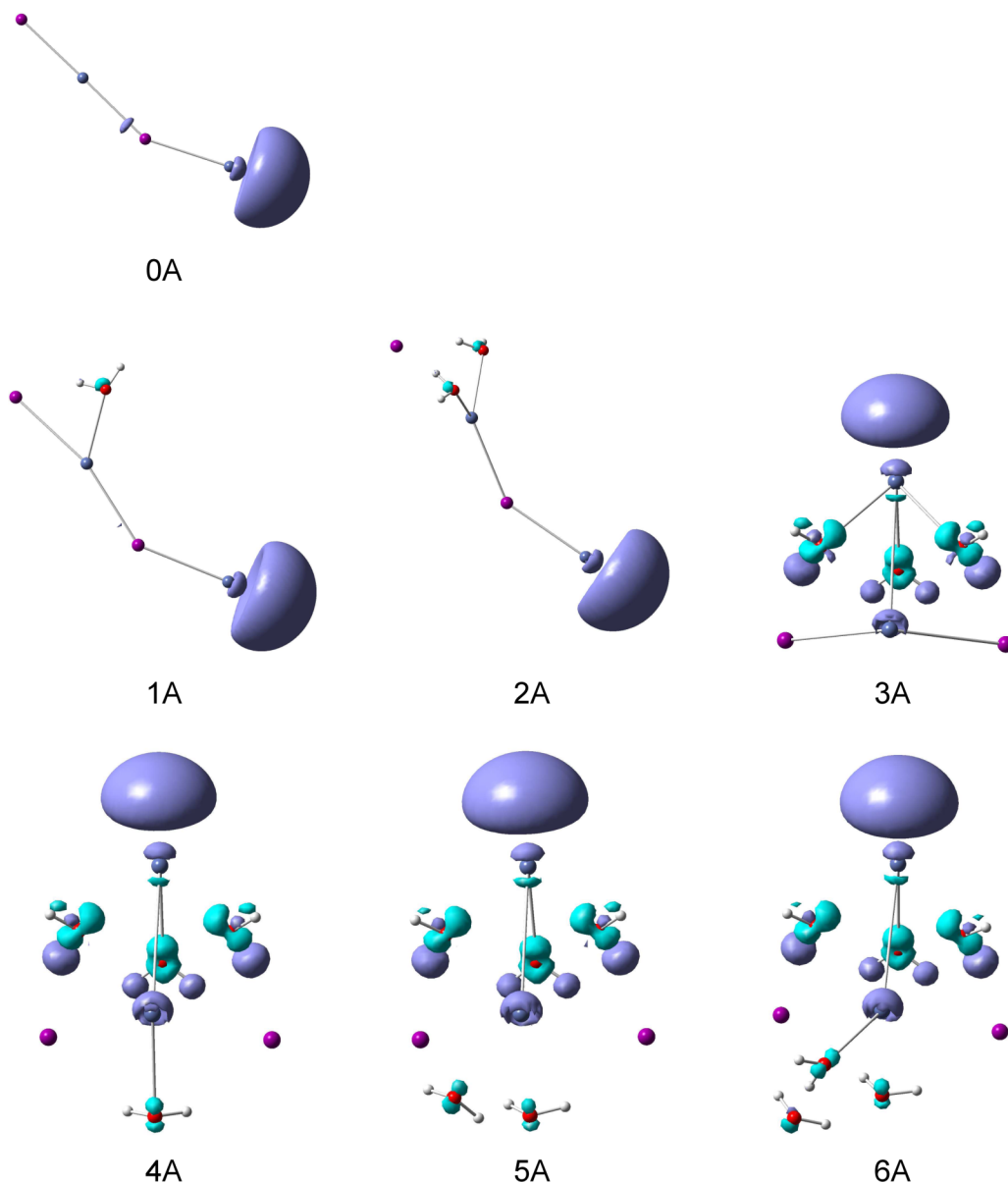


FIG. 7. Electron density differences between the most stable isomers of $(\text{KI})_2^-(\text{H}_2\text{O})_n$ ($n = 0-6$) clusters and their corresponding neutrals at the anionic structures. The blue isosurfaces (isovalue = 0.0011 a.u.) correspond to electron density increase while the light green isosurfaces (isovalue = 0.0011 a.u.) correspond to electron density decrease.

densities of these regions are increased, which is in agreement with the NPA analyses. The excess electron on K2 weakens the interactions between K2 and I atoms, in agreement with the separation of K2 atom from the other part of $(\text{KI})_2^-$ unit by water in $(\text{KI})_2^-(\text{H}_2\text{O})_3$.

C. Interaction analyses

We conducted reduced density gradient (RDG) analysis for $(\text{KI})_2^-(\text{H}_2\text{O})_n$ clusters to investigate the interactions among K^+ , I^- , and water, and displayed the gradient isosurfaces in Figure 8. For $(\text{KI})_2^-(\text{H}_2\text{O})_{1,2}$, the disks between the middle K atom and its adjacent O atoms of water are light blue whereas the regions between the terminal I atom and the neighboring H atoms of water are green, revealing that the K^+ -water interactions are stronger than the I^- -water interactions. For $(\text{KI})_2^-(\text{H}_2\text{O})_6$, the regions between the I atoms and the

adjacent H atoms of water show a color variation from green to light blue with the increasing number of water molecules, indicating an increasing electrostatic attraction. Particularly, for $(\text{KI})_2^-(\text{H}_2\text{O})_5$ and $(\text{KI})_2^-(\text{H}_2\text{O})_6$, the regions of water-water are blue, indicating there are strong $\text{O}-\text{H}\cdots\text{O}$ hydrogen bonds.

With the aim of comparison, we also analyzed the bonding and electronic properties of $(\text{KI})_2^-(\text{H}_2\text{O})_n$ clusters with the quantum theory of atoms in molecules (QTAIM) techniques, and obtained the electron density (ρ) at the (3, -1) bond critical points (BCP), the sign of its Laplacian ($\nabla^2\rho$), and total energy density (H). At the BCP, the K^+-I^- , $\text{H}-\text{I}$, $\text{O}-\text{K}$, and $\text{O}-\text{H}$ bonds have a low ρ (<0.015 a.u.), positive $\nabla^2\rho$ (≥ 0.023 a.u.), and H density (≥ 0.001 a.u.) (see Table S3 and Figure S5 in the [supplementary material](#)), indicating the interactions are dominated by the concentrated charge in the separated atomic basins rather than that in the internuclear

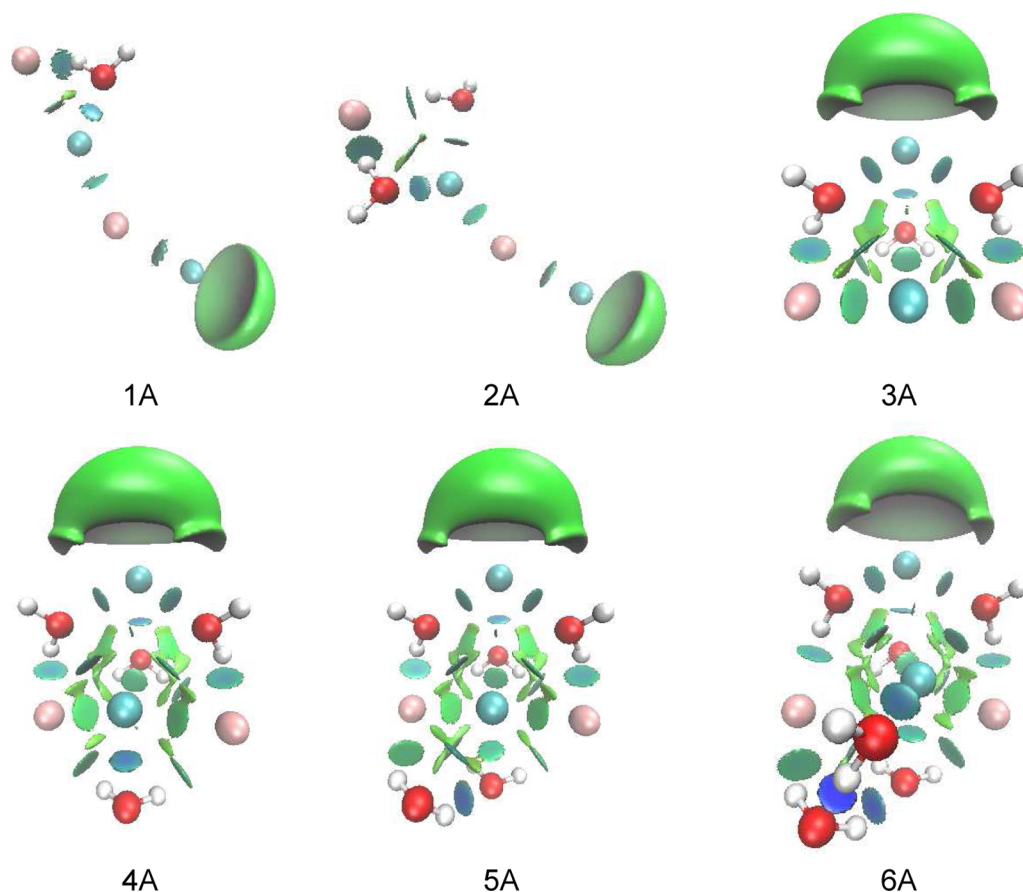


FIG. 8. Gradient isosurfaces ($s=0.6$ a.u.) for the most stable isomer of $(\text{KI})_2^-(\text{H}_2\text{O})_n$ ($n=1-6$) clusters. The surfaces are colored on a blue-green-red scale according to values of $\text{sign}(\lambda_2)\rho$, ranging from -0.022 to 0.02 a.u. Blue indicates strong attractive interactions, and red indicates steric clash.

region. These interactions are usually considered as typical closed-shell interactions.

D. $(\text{KI})_2^{-/0}(\text{H}_2\text{O})_n$ versus $(\text{NaI})_2^{-/0}(\text{H}_2\text{O})_n$

The most stable structure of bare $(\text{KI})_2^-$ has a chain structure with a $\angle\text{KIK}$ angle of 153.2° , which is larger than the corresponding $\angle\text{NaINa}$ angle in $(\text{NaI})_2^-$ (122.5°).³⁶ This probably is because the excess electron is more delocalized in $(\text{KI})_2^-$ than that in $(\text{NaI})_2^-$ and the attraction of I1-K2 is weaker. The most stable structures of both $(\text{KI})_2^-(\text{H}_2\text{O})$ and $(\text{NaI})_2^-(\text{H}_2\text{O})$ can be considered as deriving from the corresponding bare $(\text{MI})_2^-$ ($\text{M} = \text{K}, \text{Na}$) via M-O and I-H interactions. For the most stable structure of $(\text{KI})_2^-(\text{H}_2\text{O})_2$, the K1-I1 distance is longer than that in bare $(\text{KI})_2^-$ by 0.45 \AA , significantly less than the increasing of the corresponding Na1-I1 distance (1.76 \AA) in $(\text{NaI})_2^-(\text{H}_2\text{O})_2$.³⁶ In the most stable structure of $(\text{KI})_2^-(\text{H}_2\text{O})_3$, the $(\text{KI})_2^-$ unit shows a pyramid-shaped framework (Figure 3), while in the most stable structure of $(\text{NaI})_2^-(\text{H}_2\text{O})_n$, the $(\text{NaI})_2^-$ unit remains as an L shape like that in $(\text{NaI})_2^-(\text{H}_2\text{O})_n$ ($n = 1, 2$).³⁶ For the larger $(\text{KI})_2^-(\text{H}_2\text{O})_n$ and $(\text{NaI})_2^-(\text{H}_2\text{O})_n$ clusters with $n = 4-6$, the most stable structures of them have pyramid-shaped framework of $(\text{MI})_2^-$ and similar interactions between M^+-I^- , cation-water, anion-water, and water-water. From Figure 9(a), in $(\text{KI})_2^-(\text{H}_2\text{O})_n$, the K-I distances have a significant elongation when the number of water molecules

increased to 3 in $(\text{KI})_2^-(\text{H}_2\text{O})_n$; however, in $(\text{NaI})_2^-(\text{H}_2\text{O})_n$,³⁶ the abrupt increase of Na-I distance occurs at $n = 2$. This reveals that the Na^+ is more easily to be separated than K^+ .

Comparison of the neutral $(\text{KI})_2(\text{H}_2\text{O})_n$ and $(\text{NaI})_2(\text{H}_2\text{O})_n$ clusters shows that they have similar structure characteristic. Both of them have a ring $(\text{MI})_2$ unit and similar $(\text{MI})_2$ -water interactions at $n \leq 3$. Figure 9(b) shows that one of the M-I distances increases abruptly and an I^- is first separated from the other part of the $(\text{MI})_2$ unit when the number of water molecules reaches 4 in both $(\text{KI})_2(\text{H}_2\text{O})_n$ and $(\text{NaI})_2(\text{H}_2\text{O})_n$. Additionally, it is noteworthy that, in Figure 9(b), the K-I distances of $(\text{KI})_2(\text{H}_2\text{O})_n$ at $n = 4-6$ are elongated less significantly by the water molecules (smaller $d_{\text{M-I}}/d_{\text{MI}}^0$) than the Na-I distances of $(\text{NaI})_2(\text{H}_2\text{O})_n$, which is in agreement with what is observed for their anionic counterparts. There might be a few reasons for that. First, the K-I bond strength (325.1 kJ/mol) is stronger than the Na-I bond strength (304.2 kJ/mol). The second is that Na^+ has smaller size and higher surface charge density, so that the hydration of Na^+ is stronger than that of K^+ . The third is that the size of K^+ is closer to that of I^- comparing to that between Na^+ and I^- , and the similar sizes between K^+ and I^- make them have similar water affinities; therefore, the K^+-I^- pair is more difficult to be separated. This is consistent with the proposed law of matching water affinities reported by Collins,^{8,13} that is to say that ionic radius close to each other prefers to form ion pairs.

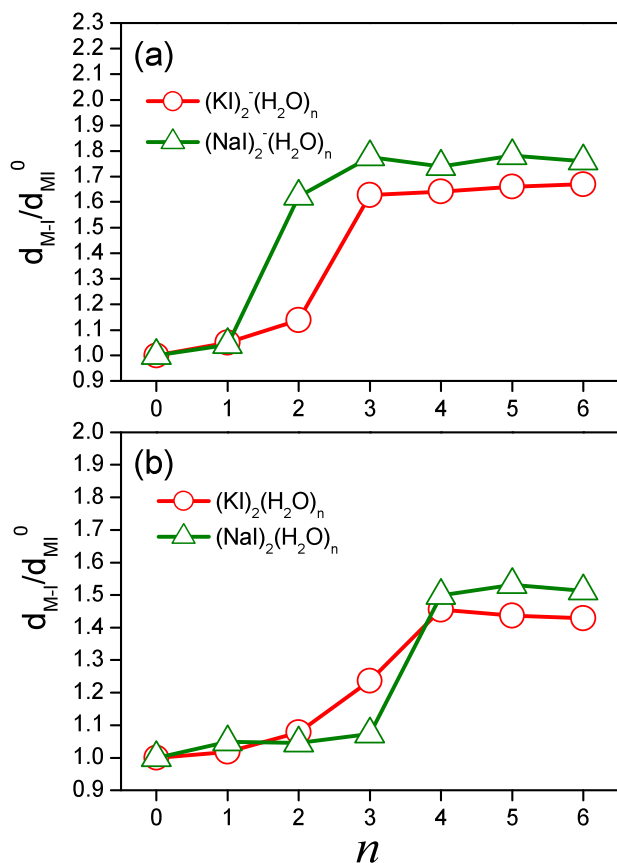


FIG. 9. Evolution of the main M–I distances versus n in the most stable isomers of anionic and neutral $(\text{KI})_2(\text{H}_2\text{O})_n$ and $(\text{NaI})_2(\text{H}_2\text{O})_n$ ($n = 0-6$). d_{M-I} is the main M–I distance, and d_{M-I}^0 is the M–I distance for $n = 0$.

V. CONCLUSIONS

We measured the photoelectron spectra of $(\text{KI})_2^-(\text{H}_2\text{O})_n$ ($n = 0-3$) and conducted *ab initio* calculations on $(\text{KI})_2^-(\text{H}_2\text{O})_n$ anions and their corresponding neutrals up to $n = 6$. The bare $(\text{KI})_2^-$ has a chain shaped structure with a $\angle\text{KIK}$ angle of 153.2° . In addition to the chain-shaped $(\text{KI})_2$ unit, the pyramid-shaped $(\text{KI})_2$ unit shows up in the low-lying isomers of $(\text{KI})_2^-(\text{H}_2\text{O})$ and $(\text{KI})_2^-(\text{H}_2\text{O})_2$. Two types of spectral features exist in the experimental spectra of $(\text{KI})_2^-(\text{H}_2\text{O})$ and $(\text{KI})_2^-(\text{H}_2\text{O})_2$, indicating that two types of isomers coexist, in which the high EBE feature corresponds to hydrated chain-like $(\text{KI})_2^-$ while the low EBE feature corresponds to hydrated pyramidal $(\text{KI})_2^-$. The pyramidal configuration becomes dominant with increasing number of water molecules. In $(\text{KI})_2^-(\text{H}_2\text{O})_3$, the K–I distances have a rapid elongation and a K atom is first separated out from the pyramid-shaped $(\text{KI})_2^-$ unit. As for the neutrals, the bare $(\text{KI})_2$ has a rhombus structure, and the structures of $(\text{KI})_2(\text{H}_2\text{O})_n$ are evolved from the rhombus $(\text{KI})_2$ unit. At $n = 4$, the K–I distances have significant increment and one of the I atoms prefers to leave the $(\text{KI})_2$ unit. The RDG analyses show that the K^+ -water interactions are dominant when the first and second water molecules interact with $(\text{KI})_2^-$; then, the I^- -water and water-water interactions are considerably enhanced with the increasing number of water molecules. The topological analyses (AIM) indicate that the K^+-I^- , H–I, O–K, and O–H interactions can be considered as closed-shell interactions.

The comparison of $(\text{KI})_2(\text{H}_2\text{O})_n$ and $(\text{NaI})_2(\text{H}_2\text{O})_n$ indicates that it is slightly more difficult to pry apart $(\text{KI})_2$ than $(\text{NaI})_2$ via hydration, which is in agreement with the lower solubility of KI compared to that of NaI.

SUPPLEMENTARY MATERIAL

See the [supplementary material](#) for the K–I distances of $(\text{KI})_2^{-/0}(\text{H}_2\text{O})_n$ ($n = 0-6$) calculated with the MP2 method, the results of QTAIM calculations, the low-lying isomers of $(\text{KI})_2(\text{H}_2\text{O})_n^{-/0}$ ($n = 0-6$) with the LC- ω PBE method, and the NPA charge distributions of the most stable isomers of $(\text{KI})_2^-(\text{H}_2\text{O})_n$ ($n = 0-6$) and their corresponding neutrals.

ACKNOWLEDGMENTS

R.Z.L. thanks the National Natural Science Foundation of China (NSFC, Grant No. 21301134), Postdoctoral Science Foundation of China (No. 2015M572545), and Open Fund of Beijing National Laboratory for Molecular Sciences (No. 2013003) for the support. W.J.Z. and Y.Q.G. acknowledge the National Natural Science Foundation of China (NSFC, Grant Nos. 21543007 and 21573006) and the Beijing National Laboratory for Molecular Sciences for the financial support. Some of the theoretical calculations were conducted on the ScGrid and DeepComp 7000 of the Supercomputing Center, Computer Network Information Center of Chinese Academy of Sciences.

- J. L. Thomas, A. Jimenez-Aranda, B. J. Finlayson-Pitts, and D. Dabdub, *J. Phys. Chem. A* **110**, 1859 (2006).
- S. W. Hunt, M. Roeselová, W. Wang, L. M. Wingen, E. M. Knipping, D. J. Tobias, D. Dabdub, and B. J. Finlayson-Pitts, *J. Phys. Chem. A* **108**, 11559 (2004).
- K. W. Oum, M. J. Lakin, D. O. DeHaan, T. Brauers, and B. J. Finlayson-Pitts, *Science* **279**, 74 (1998).
- D. A. Turtton, J. Hunger, G. Hefter, R. Buchner, and K. Wynne, *J. Chem. Phys.* **128**, 161102 (2008).
- C. L. D. Gibb and B. C. Gibb, *J. Am. Chem. Soc.* **133**, 7344 (2011).
- K. D. Collins and M. W. Washabaugh, *Q. Rev. Biophys.* **18**, 323 (1985).
- W. J. Xie and Y. Q. Gao, *J. Phys. Chem. Lett.* **4**, 4247 (2013).
- K. D. Collins, *Methods* **34**, 300 (2004).
- Y. Zhang and P. S. Cremer, *Curr. Opin. Chem. Biol.* **10**, 658 (2006).
- R. L. Baldwin, *Biophys. J.* **71**, 2056 (1996).
- D. J. Tobias and J. C. Hemminger, *Science* **319**, 1197 (2008).
- K. D. Collins, G. W. Neilson, and J. E. Enderby, *Biophys. Chem.* **128**, 95 (2007).
- K. D. Collins, *Biophys. J.* **72**, 65 (1997).
- Y. Zhou, J. H. Morais-Cabral, A. Kaufman, and R. MacKinnon, *Nature* **414**, 43 (2001).
- H. M. Lee, P. Tarakeshwar, J. Park, M. R. Kolaski, Y. J. Yoon, H.-B. Yi, W. Y. Kim, and K. S. Kim, *J. Phys. Chem. A* **108**, 2949 (2004).
- C. Krekeler, B. Hess, and L. D. Site, *J. Chem. Phys.* **125**, 054305 (2006).
- A. Bankura, V. Carnevale, and M. L. Klein, *J. Chem. Phys.* **138**, 014501 (2013).
- Y. Liu, H. Lu, Y. Wu, T. Hu, and Q. Li, *J. Chem. Phys.* **132**, 124503 (2010).
- T. W. Whitfield, S. Varma, E. Harder, G. Lamoureux, S. B. Rempe, and B. Roux, *J. Chem. Theory Comput.* **3**, 2068 (2007).
- T. Ikeda, M. Boero, and K. Terakura, *J. Chem. Phys.* **126**, 034501 (2007).
- G. Sciaini, R. Fernandez-Prini, D. A. Estrin, and E. Marceca, *J. Chem. Phys.* **126**, 174504 (2007).
- A. C. Olleta, H. M. Lee, and K. S. Kim, *J. Chem. Phys.* **126**, 144311 (2007).
- G. W. Neilson and N. Skipper, *Chem. Phys. Lett.* **114**, 35 (1985).
- A. K. Soper and K. Weckström, *Biophys. Chem.* **124**, 180 (2006).
- R. Mancinelli, A. Botti, F. Bruni, M. A. Ricci, and A. K. Soper, *J. Phys. Chem. B* **111**, 13570 (2007).

- ²⁶V.-A. Glezakou, Y. Chen, J. L. Fulton, G. K. Schenter, and L. X. Dang, *Theor. Chem. Acc.* **115**, 86 (2006).
- ²⁷J. Mähler and I. Persson, *Inorg. Chem.* **51**, 425 (2012).
- ²⁸Y. L. Jeyachandran, F. Meyer, A. Benkert, M. Bär, M. Blum, W. Yang, F. Reinert, C. Heske, L. Weinhardt, and M. Zharnikov, *J. Phys. Chem. B* **120**, 7687 (2016).
- ²⁹F. Li, J. S. Yuan, D. C. Li, S. Y. Li, and Z. Han, *J. Mol. Struct.* **1081**, 38 (2015).
- ³⁰J. S. Yuan, Z. Y. Liu, F. Li, and S. Y. Li, *Acta Phys.-Chim. Sin.* **32**, 1143 (2016).
- ³¹S. Suzer and L. Andrews, *Chem. Phys. Lett.* **140**, 300 (1987).
- ³²A. T. Blades, M. Peschke, U. H. Verkerk, and P. Kebarle, *J. Am. Chem. Soc.* **126**, 11995 (2004).
- ³³H. Ke, C. van der Linde, and J. M. Lisy, *J. Phys. Chem. A* **119**, 2037 (2015).
- ³⁴D. J. Miller and J. M. Lisy, *J. Am. Chem. Soc.* **130**, 15381 (2008).
- ³⁵R. J. Cooper, T. M. Chang, and E. R. Williams, *J. Phys. Chem. A* **117**, 6571 (2013).
- ³⁶R.-Z. Li, G.-L. Hou, C.-W. Liu, H.-G. Xu, X. Zhao, Y. Q. Gao, and W.-J. Zheng, *Phys. Chem. Chem. Phys.* **18**, 557 (2016).
- ³⁷H.-G. Xu, Z.-G. Zhang, Y. Feng, J. Yuan, Y. Zhao, and W. Zheng, *Chem. Phys. Lett.* **487**, 204 (2010).
- ³⁸M. J. Frisch, G. W. Trucks, H. B. Schlegel, G. E. Scuseria, and M. A. Robb, *GAUSSIAN 09*, Revision D.01, Gaussian, Inc., 2009.
- ³⁹O. A. Vydrov and G. E. Scuseria, *J. Chem. Phys.* **125**, 234109 (2006).
- ⁴⁰O. A. Vydrov, J. Heyd, A. V. Krukau, and G. E. Scuseria, *J. Chem. Phys.* **125**, 074106 (2006).
- ⁴¹O. A. Vydrov, G. E. Scuseria, and J. P. Perdew, *J. Chem. Phys.* **126**, 154109 (2007).
- ⁴²M. Head-Gordon, J. A. Pople, and M. J. Frisch, *Chem. Phys. Lett.* **153**, 503 (1988).
- ⁴³M. J. Frisch, M. Head-Gordon, and J. A. Pople, *Chem. Phys. Lett.* **166**, 275 (1990).
- ⁴⁴M. J. Frisch, M. Head-Gordon, and J. A. Pople, *Chem. Phys. Lett.* **166**, 281 (1990).
- ⁴⁵M. Head-Gordon and T. Head-Gordon, *Chem. Phys. Lett.* **220**, 122 (1994).
- ⁴⁶W. R. Wadt and P. J. Hay, *J. Chem. Phys.* **82**, 284 (1985).
- ⁴⁷K. L. Schuchardt, B. T. Didier, T. Elsethagen, L. Sun, V. Gurumoorthi, J. Chase, J. Li, and T. L. Windus, *J. Chem. Inf. Model.* **47**, 1045 (2007).
- ⁴⁸G. D. Purvis and R. J. Bartlett, *J. Chem. Phys.* **76**, 1910 (1982).
- ⁴⁹G. E. Scuseria, C. L. Janssen, and H. F. Schaefer, *J. Chem. Phys.* **89**, 7382 (1988).
- ⁵⁰D. Rappoport and F. Furche, *J. Chem. Phys.* **133**, 134105 (2010).
- ⁵¹R. F. W. Bader, *Atoms in Molecules* (Wiley Online Library, 1990).
- ⁵²R. F. W. Bader, *Chem. Rev.* **91**, 893 (1991).
- ⁵³E. R. Johnson, S. Keinan, P. Mori-Sánchez, J. Contreras-García, A. J. Cohen, and W. Yang, *J. Am. Chem. Soc.* **132**, 6498 (2010).
- ⁵⁴T. Lu and F. Chen, *J. Comput. Chem.* **33**, 580 (2012).
- ⁵⁵Y. Yang, L. Bloomfield, C. Jin, L. Wang, and R. Smalley, *J. Chem. Phys.* **96**, 2453 (1992).
- ⁵⁶G.-L. Hou, G. Feng, L.-J. Zhao, H.-G. Xu, and W.-J. Zheng, *J. Phys. Chem. A* **119**, 11154 (2015).